*ASSOCIAÇÃO BRASILEIRA DE ENERGIA NUCLEAR – ABEN*
*2019 International Nuclear Atlantic Conference - INAC 2019*
*Santos, SP, Brazil, October 21-25, 2019*

Agência Brasileira do ISBN
ISBN 978-85-99141-08-3
9 788599 141083

# CHEMICAL AND PHYSICAL ANALYSIS OF SANDSTONE ROCK FROM BOTUCATU FORMATION

**João Carlos Corrêa[1], Rafael H. L. Garcia[1], Rodrigo S. dos Santos[1], Rafael A. Amadeu[1], Thiago L. S. Bernardes[1], Alexandre F. Velo[1], Diego V. S. Carvalho[1], Tarciano J. do Nascimento[2], Francisco A. Cavallaro[2], Carlos H. de Mesquita[1] and Margarida M. Hamada[1]***

[1]Instituto de Pesquisas Energéticas e Nucleares (IPEN / CNEN - SP)
Av. Professor Lineu Prestes 2242
05508-000 São Paulo, SP
mmhamada@ipen.br

[2]Universidade Cidade de São Paulo (UNICID)
R. Cesário Galero448/475
03071-000 São Paulo, SP, Brazil

## ABSTRACT

The productive capacity of the Guarani Aquifer System is subject to variations along its length, due to its complex structural and compositional heterogeneity. Several parameters may influence the quality of this reservoir rock, such as its mineralogical and textural constitution, as well as the physicochemical processes, its diagenesis is not the same throughout the aquifer, influencing the water productivity in wells in different locations. Such parameters are useful in the geoscience studies, in the elaboration of diagenetic models for the prediction of the reservoir quality. In this work, several properties of the sandstone rock from Botucatu Formation were determined, using different techniques, such as geotechnical tests, optical microscopy (MO), electron scanning microscopy (SEM), X-ray Fluorescence and X-ray diffraction. The results indicate that the studied sandstones have characteristics of the reservoir rocks, with potential for water storage.

## 1. INTRODUCTION

The Botucatu Formation is an important reservoir rock and it is located at the top of the Guarani Aquifer. Reservoir rocks are rocks characterized by suitable porosity and permeability to contain a fluid. Porosity is the relationship between the volume of voids and the total volume of a rock and permeability is the ability of a fluid to flow through a rock. (Caetano-Chag, 1993).

The Guarani Aquifer is the largest underground freshwater spring in the world. It is located mostly in Brazil - South and Southeast, and also covers Paraguay, Uruguay and Argentina, occupying an area of approximately 1 million km$^2$. The thickness of this aquifer may reach

450 meters in the central part of the Paraná Basin, in which it is contained. Often there is contact, in its upper part, with basalts of the Serra Geral formation. The origin of the water in the Guarani aquifer, in great part, comes from the percolation of meteoric waters over a period of time of thousands of years, in the regions of outcrops.

The Botucatu Formation consists mainly of quartz sandstones of fine to medium granulation, of red, pink or light yellow coloration, well selected, mature, and it may contain altered feldspar, cemented by silica or iron oxide, which gives it a pink coloration (Bigarella, 1967). As a characteristic structure of these sandstones, large tangential cross stratification occurs. (Caetano-Chag,1992).

The water stored in the Guarani Aquifer, mainly by the Botucatu formation, is widely used in the supply of hundreds of cities located above it, by means of wells of varied depths. The water quality of this aquifer is at risk of being impaired, mainly by inadequate agricultural, industrial and waste disposal activities. The water stored in the Guarani aquifer, mostly by the Botucatu formation, is widely used in the supply of hundreds of cities located above that, by means of wells of varied depth. The water quality of this aquifer is at risk of being impaired, mainly by inadequate agricultural, industrial and waste disposal activities.

The Guarani Aquifer System (GAS), because it is of complex origin, cannot be restricted only to the hydrogeological aspect. The quality of the aquifer depends on: (a) the prevailing climatic conditions of the recharge area, (b) the interaction of the infiltrated water with the rock, (c) the sedimentary characteristics of the sandstones (depositional conditions, diagenetic modifications and tectonic compartmentation).

The interest of the society in the use and protection of underground water sources has been widened due to pollution and accelerated scarcity of surface water resources. Despite its transboundary extension, it is in the State of São Paulo, the most industrialized and populous region, that the Guarani Aquifer is most intensively used, thus concentrating the largest number of tubular wells. Part of these wells is intended for public supply (Chang 2006).

In São Paulo, the Guarani Aquifer System (Figure 2) is delimited at the bottom and at the top by two aquitards, respectively the Cretaceous volcanic rocks of the Serra Geral Formation and the Permian pelitic rocks of the Passa Dois Group (Corumbataí, Teresina, Rastro River Formations). Although regionally it constitutes a fractured aquifer, the Serra Geral imposes deep confinement conditions to the pre-volcanic sandy sedimentary set, determining the SAG artesian incidence in much of the west of São Paulo.

Due to its complex structural and compositional heterogeneity, the productive capacity of the GAS is subject to variations along its length (Machado, 2005). Several parameters may influence the quality of this reservoir, such as its mineralogical and textural constitutions, as well as the physicochemical processes during its diagenesis are not the same throughout the aquifer, influencing the water productivity in wells, in different locations. Such parameters are useful in the geoscience studies in the elaboration of diagenetic models for the prediction of the reservoir quality. Several studies have been carried out in the literature for the physical, physical-chemical and structural characterization of reservoir rocks that make up the GAS, such as the Botucatu Formation (Wu & Caetano-Chang (1992), Caetano-Chang & Wu ), Caetano-Chang & Wu (2003), Gesicki (2007) and Rocha (2017), SOARES (1972). However, due to the complexity and heterogeneity in their structures and compositions, according to

their location, studies for knowledge about the reservoir rocks of each region need to be performed. This work aims to increase the information about the properties of the Botucatu Formation reservoir rock from the Guarani Aquifer System, using different geotechnical assays, such as the determination of the shear velocity, permeability and plasticity limit. Also, analytical techniques for its characterization, such as the Scanning Electron Microscope (SEM), 2007) (LIU, 2019), Fluorescence and X-ray Diffraction (PETERSON, 2018) (SCAPIN, 2003) were used.

## EXPERIMENTAL PART

Samples of Botucatu Formation sandstones were collected from the area located 180 km from the capital of. (West), at kilometer 190 of the Castelo Branco Highway, 11 km from the city of Bofete (Lat 23,168,778 °, lon - 48.333111). Samples were collected in mid-January 2018 following the standard NBR 16434/2015, which describes recommended procedures for the collection, handling and preparation of solid waste, soil and sediment samples.

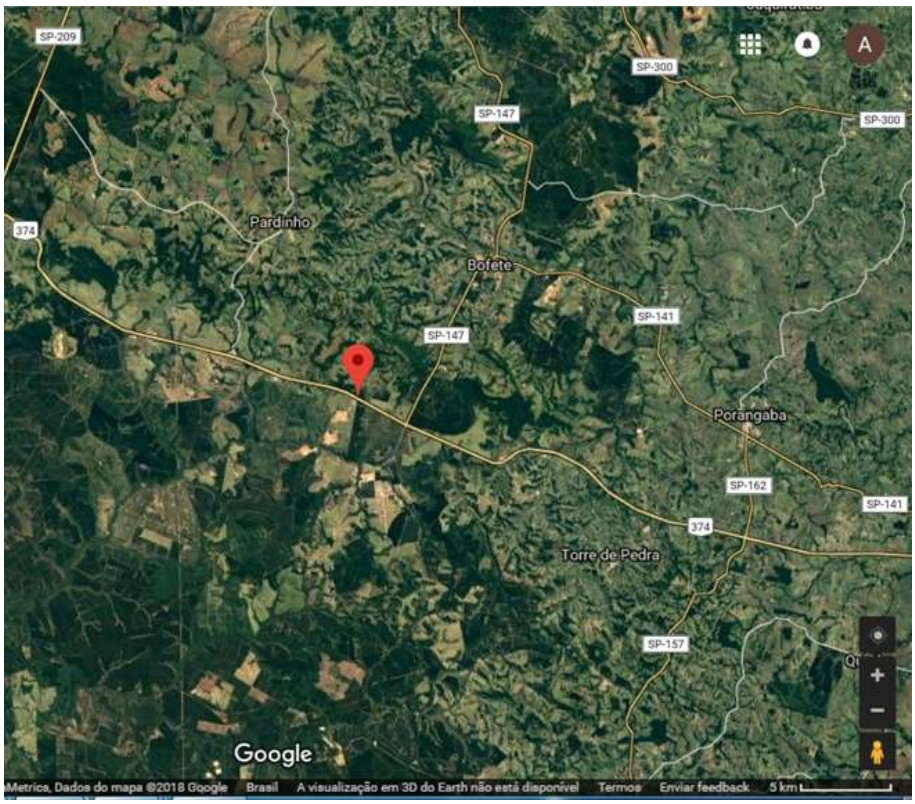


Source: Google.com.br, 2018

**Figure 3 – Location of the sample collection area of the Botucatu Formation rock (km 190 of the Castelo Branco highway, State of São Paulo).**

Next, these rock samples were characterized by geotechnical tests and analytical techniques,

### 3.1. Geotechnical assays

3.1.1 Calculation of shear wave velocity by means of piezoelectric elements – Assays with Bender Elements.

In order to calculate the shear wave rate, bender elements were used to convert electric energy into mechanical energy or vice versa, the so-called piezoelectricity, which allows piezoelectric transducers to act as actuators or sensors and, in most cases, the same transducer may perform both functions (Ferreira, 2003).

The bender elements are small rectangular piezo-ceramic plates that undergo flexion when excited by electric pulses or generate electric pulses when flexed. A length of 3 to 9 mm of these plates is balanced, so that they are inserted into the soil to be tested. The bender elements work in pairs, being a transmitter element and a receiver, and are positioned on opposite faces of the test body (Squeglia, 2009).

For the test with the bender elements, it is initially necessary to carry out the calibration of the transducers. To do this, the time delay measurement is performed regularly, which consists of measuring the propagation time of the wave by means of the contact between the two transducers used for transmission and reception. It is recommended that the time delay and the measurement of the speed of the wave in the ground may be accomplished in diverse frequencies, and the data to be considered in the calculation should be the average between the obtained values. Figure 2 illustrates the bender elements transducer calibration scheme using a Minipa MVB-DSO digital oscilloscope, while Figure 3 shows the test body used in the bender elements assay.

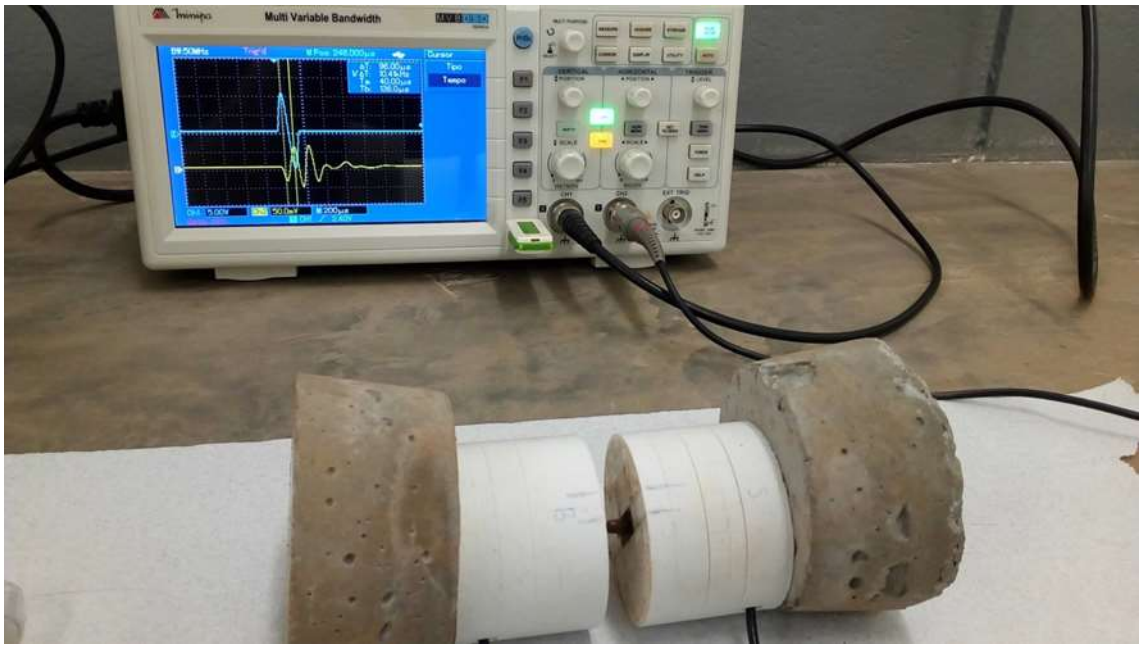


Figure 2: Illustrative picture of the calibration scheme of bender elements transducers.

The time delay data measured in the experiments are shown in Table 1:

Table 1: Time delay results for each of the Frequency values used.

| Frequency | *Time delay* (μs) |
|---|---|
| 5 kHz | 96-100 |
| 7 kHz | 84-88 |
| 10 kHz | 72-76 |
| 12 kHz | 66-72 |
| 15 kHz | 62-64 |
| 20 kHz | 60-64 |

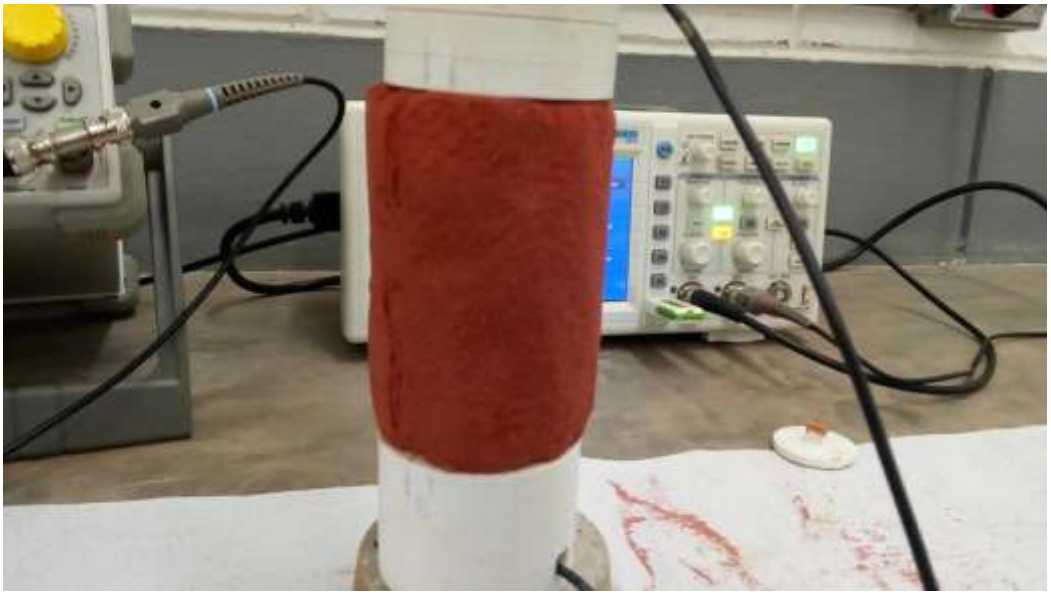

Figure 3: Probe used in the bender elements test

For the stimulation of the movement in the piezoelectric transducer, in the experiments with the bender elements, a wave generator model Minipa MFG-4205, was used. A Minipa MVB-DSO digital oscilloscope was used for receiving and observing the wave propagated in the specimen and captured by the receiver element, the data have been used to calculate the propagation time of the wave. The experimental apparatus for testing the bender elements is shown in Figure 4.

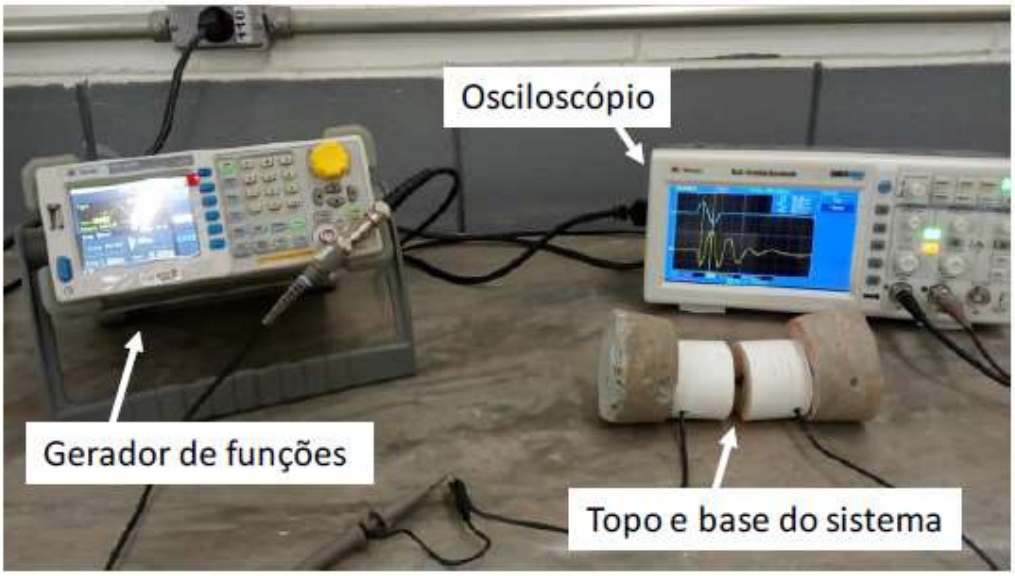


Figure 4. Experimental apparatus for assay with bender elements
(Osciloscopy, Function generator, System top and bottom)

In order to calculate the shear wave velocity, two considerations were taken into account: (1) the distance to be used in the calculations considered the distance between the ends of the bender elements, as recommended by Viggiani and Atkinson (1995) and 2) the time to propagate the wave (t) was considered as being the first peak of the sine wave transmitted to the first peak, after the signal deflection received (peak-to-peak method), what is generally observed in shear waves.

The calculation of the shear wave velocity across the soil, given by equation (1), considers that the length traveled by it corresponds to the distance between the ends of the transmitting and receiving element (Lt) (Viggiani and Atkinson, 1995: Dyvik and Madshus, 1985), even if the time taken in this path (t) is given by the interval between the emission and reception of the wave.

Thus, the relationship between these two quantities provides the propagation velocity of the shear wave within the soil.

$$Vs = Lt/t \qquad (1)$$

The bender elements tests were performed under several frequency variations. Thus, both the assay and the calibration were performed with the generation of a single sine wave, with amplitude of 20V peak-to-peak, along with six different frequencies, being the same of the calibration step.

### 3.1.2 Atterberg Limits by Casagrande Method

The Atterberg Boundaries, methods of evaluating the nature of soils, were created by Albert Atterberg. By means of a series of tests, the Liquidity Limits – WL were defined (state that only presents water content, and above this value the soil behaves as a fluid) and Plasticity -

Wp (state in which the soil presents water content below this value, behaving as solid). (Pinto, 2006). The Brazilian standard NBR-6459/84 regulates this test. With these two limits the Plasticity Index (IP = WL-Wp) is determined.

The liquidity test was performed using the Casagrande method, using the apparatus of the same name, shown in Figure 5, with which blows were applied by letting the shell of the apparatus fall from a standard height so that it closes at the end with two strokes. (DAS e SOBHAN, 2015) (PINTO, 2006).

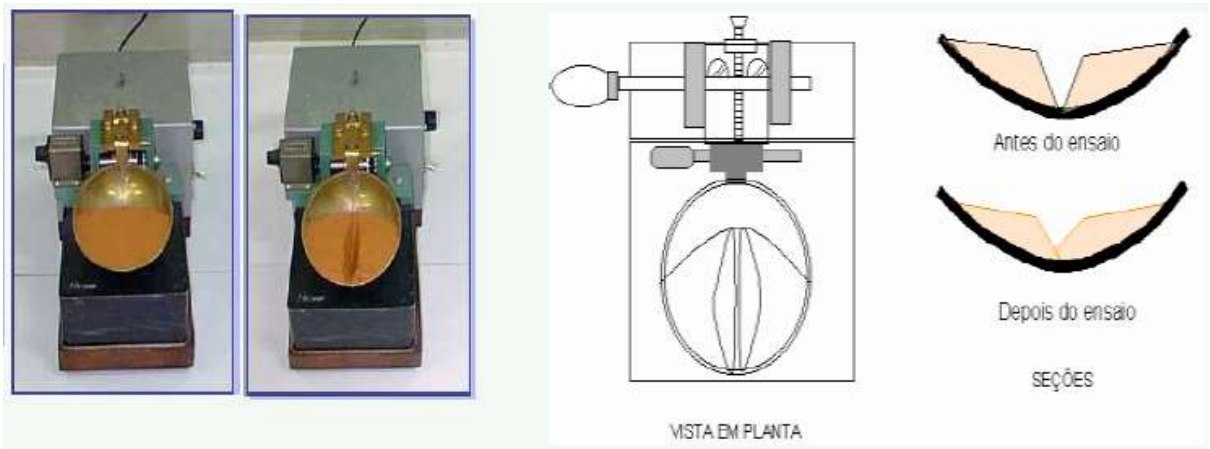


Figure 5. Picture of the apparatus of Casagrande (a), the scheme of Casagrande method (b) and (c) schematic sections of the shells before and after the test.

The assay was repeated five times by changing the unit. The WL value has been determined by projecting the number of standard strokes (25) on the interpolated line, through the points determined in the graph (Figure 6).

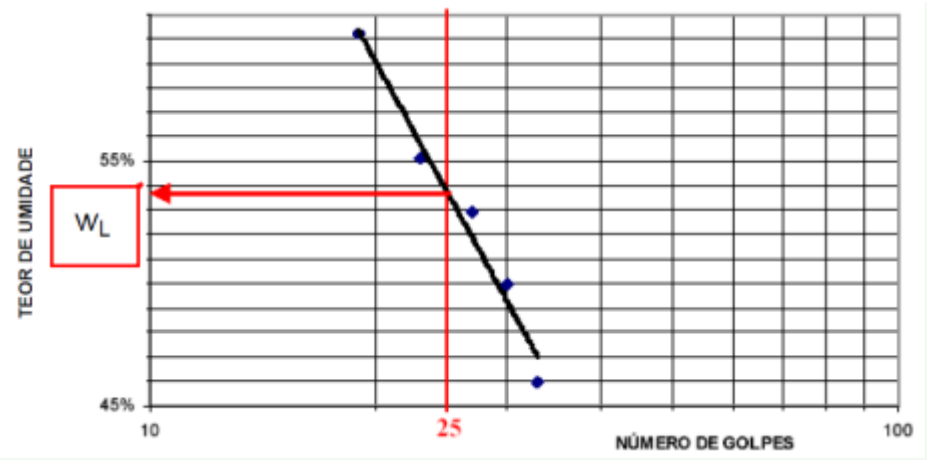


Figure 6 – Result of the moisture content as a function of the blow number to determine the liquidity limit.

The plasticity limit (Wp) is obtained with the lowest moisture content with which a 3 mm diameter cylinder is molded, rolling with the palm of the hand on a ground glass plate (Figure

7). When this cylinder breaks, it is weighed and kiln dried, and then weighed again to obtain the moisture.

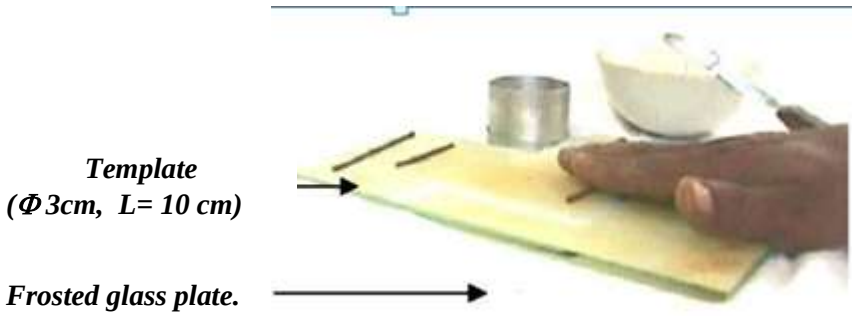


Figure 7 – Illustrative picture of obtaining the plasticity limit (Wp).

These tests help to define the limits of soil consistency. The term consistency is used to determine a physical state, that is, to know the degree of bonding between the particles of the substances. When used in thin or cohesive soils, consistency is related to the amount of water in the soil, i.e., the moisture content (PINTO, 2006).

3.1.3. Normal Proctor Assay

For the normal Proctor assay, the soil was compacted into a mold having a volume of 944 $m^3$, the mold diameter being 101.6 mm (Figure 8 a, b and c). During the laboratory test, the mold was attached to a support plate at the bottom and extended to the top, as shown in Figure 6 schematic. The soil was mixed with different amounts of water, total of five trials (Figure 8d). In each test it was compacted into three equal layers, with the moisture content of compacted soil determined in the laboratory, by a socket that strikes 25 times each layer. The martelete has 2.5 kg of mass and fall height of 30.5 cm. For each test, the specific wet weight of compaction was calculated in accordance with equation 2.

According to Das and Sobhan (2015)

$$\gamma = W/V\_m \quad (2)$$

where:

W= compacted soil weight in the mold and Vm = mold volume [944 $cm^3$].

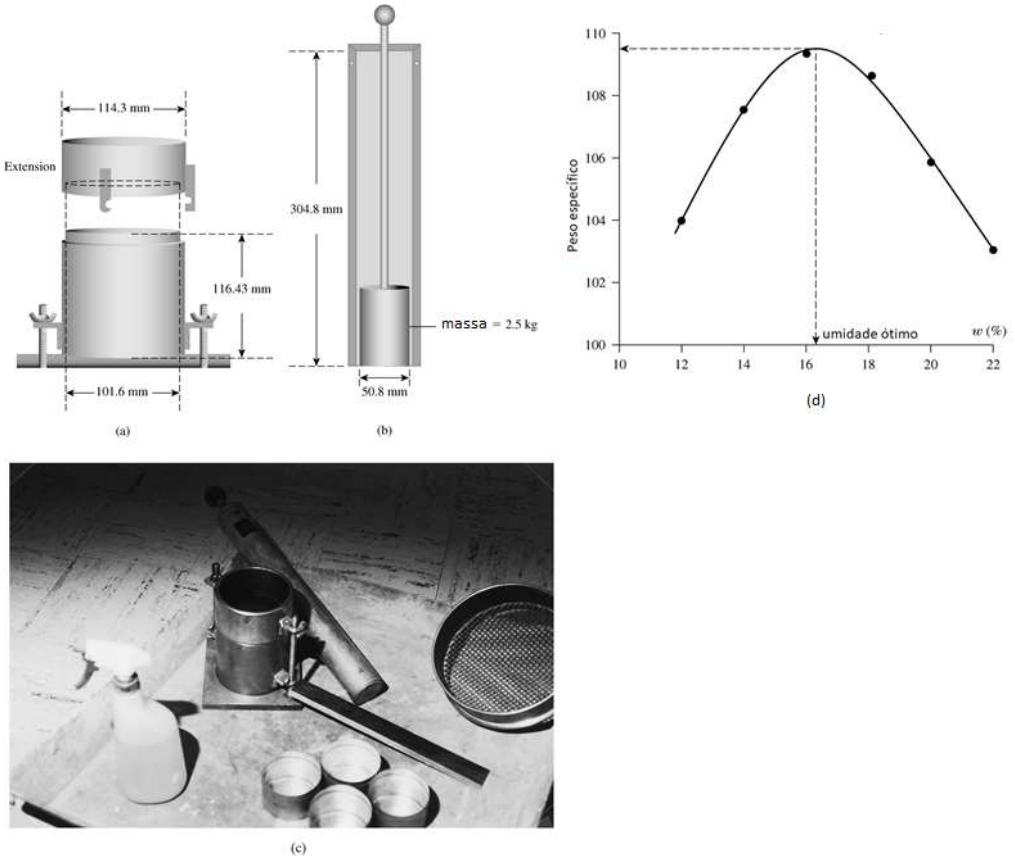


Source: DAS, 2014.

Figure 8 – Illustration of the proctor test (a and b). In (c), a photo of the test components and in (d), the graph obtained in six tests, varying the amount of moisture.

3.1.3 Permeability tests - Constant charge

The constant charge permeability measurement was performed with a typical constant load permeability test arrangement (DAS and SOBHAN, 2015), the scheme of which is shown in Figure 9. The water supply at the inlet was adjusted so that the difference between input and output remains constant, i.e, with no variation during the test period. After a constant flow had been established, the water was collected in a graduated burette (500 ml) until it reached the maximum graduation. The filling time of this volume was measured using a stopwatch, as shown in figure 9.

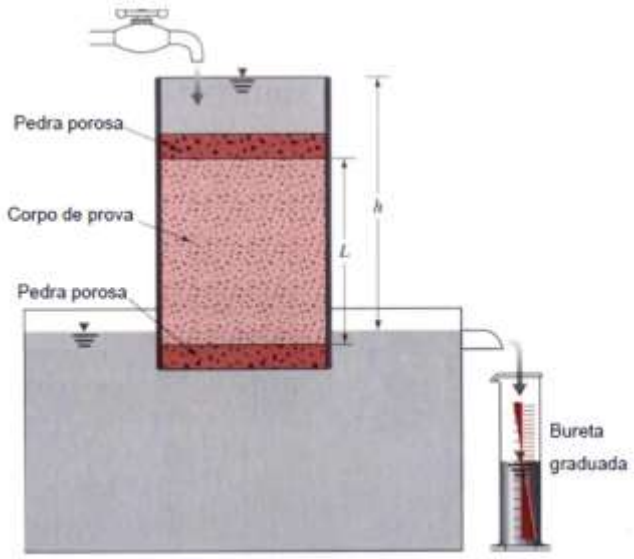


Figure 9. Scheme of the permeability test with constant load.

Source: DAS, 2014.

The total volume of water collected is expressed by equation 3:

$$V = A\left(k\frac{h}{L}\right)t, \qquad (3)$$

where:
A = cross-sectional area;
k = permeability constant;
h and L are the sample dimensions;
t = time in seconds.

Thus, the permeability constant (k) may be expressed by equation 4:

$$k = \frac{VL}{Aht} \qquad (4)$$

## 3.2 **Physical-chemical characterization of sandstone rocks.**

### 3.2.1. Analysis of the crystalline structure: X-ray diffraction (XRD)

The evaluation of the crystalline quality of the sandstone samples from Botucatu Formation was performed using the X-ray diffraction model, MULTIFLEX, brand RIGAKU. In this

process, the directions in which the planes of the crystal are preferentially oriented (Miller indices) are identified. X-ray diffraction patterns were obtained in the diffractometer from CuKα radiations (2θ ranging from 20º to 60º).

The samples were sprayed in order to allow the diffraction planes of the material with specific orientation to be distributed in all directions, increasing the probability of diffraction.

3.2.2 Fluorescence of X-rays.

The qualitative and quantitative chemical composition of the collected sandstone sample was performed using the X-ray fluorescence technique and the X-ray Fluorescence Model EDX-900HS, SHIMADZU brand. X-ray fluorescence spectrometry is a technique for identifying the elements present in a sample, as well as establishing the concentration at which each element is present in the sample. In X-ray fluorescence spectrometry a high energy radiation source (gamma radiation or X radiation) causes excitation of the substance atoms to be analyzed. When an atom in the ground state is under the action of an external source of energy, it absorbs this energy, promoting electrons to more energetic levels. In this state, the atom will be in an unstable situation, called "Excited State". In nature, everything tends to seek the state of stability and, hence, the excited atom tends naturally to return to its ground state, and then occurring an emission of energy. This energy involved in the absorption is a specific characteristic of each chemical element, allowing its identification and corresponding quantification. (Beckhoff, 2006).

3.2.3. Optical Microscopy (OM) and Electron Scanning Microscopy (SEM)

Microscopy analyses were carried out to investigate the morphology of sandstones pulverized by optical microscopy and scanning electron microscopy.

Initially, the microscopic analysis was performed using a Leica microscope, model DM-750M, with magnifiers of 5 to 100 times and filters and polarization regulation, for a previous evaluation of the pulverized sandstone morphology. This technique allowed the analysis of large areas, besides being a simple, fast and inexpensive operation.

Next, the scanning electron microscopy examination was performed to verify the morphology and the elemental chemical composition. This method allows observing homogeneity and structural quality on a much larger scale (10-20,000 X) using a scanning electron microscope LX 30, from Philips.

The Scanning Electron Microscope (SEM) is a versatile device that allows structural and chemical information from various samples to be obtained. A thin beam of high energy electrons is incident on the sample surface where, when an interaction occurs, part of the beam is reflected and collected by a detector that converts this signal into BSE (or ERE) image. In this interaction, the sample emits electrons producing the SE call (secondary electrons). There is, also, the emission of X-rays providing the elemental chemical composition of a point or region of the surface and allowing the identification of practically any element present (SANTOS, 2016).

## 2. RESULTS AND DISCUSSION

The results of the wave propagation time in the sandstone soil at each point of variation of humidity, already discarded the time delay, of the 5 samples with different humidity are shown in Table 2:

Table 2: Results of the values obtained from the Propagation Time of the sandstone soil wave, as a function of the values of Frequency for each of the five samples

| | | | | | |
|---|---|---|---|---|---|
| | Samples | | | | |
| | 1 | 2 | 3 | 4 | 5 |
| **Frequency** | **Propagation Time (*t*)(μs)** | | | | |
| 5 kHz | 320 | 380 | 660 | 610 | 680 |
| 7 kHz | 324 | 384 | 656 | 606 | 660 |
| 10 kHz | 328 | 396 | 660 | 610 | 664 |
| 12 kHz | 326 | 392 | 658 | 608 | 694 |
| 15 kHz | 322 | 400 | 662 | 612 | 698 |
| 20 kHz | 332 | 0 | 664 | 614 | 700 |
| Media | 325 | 390 | 660 | 610 | 683 |

With the results of the wave propagation data, the calculation of the maximum shear modulus (Gmax) of the sandstone soil tested in each stage of humidity increase in the compaction test, using equation 1, it was performed the shear strength in the minimum deformations (0.001%) of the soil, under variations of humidity and density, which are shown in Table 3.

Table 3: Results of humidity values and maximum shear modulus (Gmax) for each of the five soil samples.

| | 1 | 2 | 3 | 4 | 5 |
|---|---|---|---|---|---|
| **Humidity (%)** | 4.94 | 5.70 | 6.26 | 9.03 | 13.10 |
| **Gmax (MPa)** | 220.30 | 182.99 | 66.62 | 63.67 | 33.98 |

In Table 4, the values of shear wave propagation velocity (Vs) associated with the data obtained in the Proctor compaction test, such as dry density ($\rho_d$), void index (e), moisture con tent (W), degree of saturation (S) and porosity ($\eta$) corresponding are summarized.

Table 4: Shear wave propagation velocity (Vs) values associated to the values of dry density ($\rho_d$), void index (e), moisture content (W), degree of saturation (S) and porosity ($\eta$ )

| Sample | $\rho_d$ (g/cm³) | e | W (%) | S (%) | $\eta$ (%) | $V_s$ (m/s) |
|---|---|---|---|---|---|---|
| 1 | 1.81 | 0.436 | 4.9 | 29.5 | 30.4 | 291.1 |
| 2 | 1.86 | 0.395 | 5.7 | 37.4 | 28.3 | 265.3 |
| 3 | 1.87 | 0.392 | 6.3 | 41.6 | 28.1 | 160.1 |
| 4 | 1.78 | 0.461 | 9.0 | 51.0 | 31.5 | 156.5 |
| 5 | 1.57 | 0.659 | 13.,1 | 51.7 | 39.7 | 114.3 |

The results of the test for the measurement of soil permeability are shown in Table 5:

Table 5: Result of the value of the permeability coefficient (k) of the soil and the parameters used in the test for the calculation of (k)

| Sample | h (cm) | $V_{water}$ ($cm^3$) | L(cm) | t(m ->s) | t (s) | (total) | k (cm/s) |
|---|---|---|---|---|---|---|---|
| 1 | 165 | 500 | 15,3 | 780 | 5,45 | 785,45 | $3{,}34_x10^{-4}$ |

The coefficient of permeability (k) obtained in the test indicates a high permeability, being a result consistent with a sandstone soil, originating from reservoir rock (PINTO, 2006).

The assay to obtain the plasticity limit was performed, however, with the impossibility of performing a 3 mm diameter cylinder molding of the respective soil, according to NBR 7180 (1984), it may be concluded that the soil is not plastic .

In the analysis of the composition of the elements present, using X-Ray Fluorescence, several elements were determined, as presented in Table 6 (A). By inference, the values of the elements in the oxide form were estimated, as also summarized in Table 6 (B) . As it may be observed in this table, the analyzed sandstone is composed mainly of $SiO_2$ (76%) and $Al_2O_3$ (20%), followed by $Fe_2O_3$ (2.3%). Other oxides identified are present in the ppm range.

Table 6: Composition of the elements (A) and the elements in the oxide form (B) present in Botucatu sandstone rock.

| Element | Concentration | Error (%) |
|---|---|---|
| Si | 74.3 % | 0.16 |
| Al | 17.5 % | 0.30 |
| Fe | 5.01 % | 0.22 |
| Tl | 1.26 % | 0.97 |
| K | 0.959 % | 1.36 |
| Ca | 0.233 % | 2.73 |
| Mg | 0.185 % | 4.29 |
| Zr | 0.137 % | 0.56 |
| Cl | 0.103 % | 6.26 |
| Zn | 549 ppm | 2.08 |
| S | 496 ppm | 7.11 |
| P | 472 ppm | 10.5 |
| Mn | 471 ppm | 4.58 |
| Ce | 447 ppm | 15.9 |
| Ag | 186 ppm | 12.4 |
| V | 129 ppm | 18.9 |
| Ru | 123 ppm | 17.4 |
| Cu | 111 ppm | 9.49 |
| Cr | 86.4 ppm | 17.20 |
| Ni | 68.1 ppm | 17.01 |
| Sr | 36.1 ppm | 38.62 |

(A)

| Element | Concentration | Error (%) |
|---|---|---|
| $SiO_2$ | 75.9 % | 0.16 |
| $Al_2O_3$ | 20.2 % | 0.30 |
| $Fe_2O_3$ | 2.29 % | 0.22 |
| $TiO_2$ | 0.698 % | 0.37 |
| $K_2O$ | 0.392 % | 1.35 |
| CaO | 0.209 % | 4.29 |
| MgO | 0.110 % | 2.78 |
| $ZrO_2$ | 540 ppm | 0.57 |
| $SO_3$ | 428 ppm | 7.11 |
| $P_2O_5$ | 378 ppm | 10.5 |
| Cl | 353 ppm | 6.26 |
| $CeO_2$ | 230 ppm | 16.9 |
| ZnO | 202 ppm | 2.08 |
| MnO | 196 ppm | 4.56 |
| $V_2O_5$ | 149 ppm | 18.9 |
| Ag | 69.8 ppm | 12.4 |
| CuO | 41.1 ppm | 9.49 |
| $Cr_2O_3$ | 39.3 ppm | 17.2 |
| Ru | 36.5 ppm | 17.4 |
| NO | 25.6 ppm | 17.0 |
| SrO | 12.4 ppm | 39.6 |

(B)

X-ray diffraction is a technique that may be applied to the investigation of sandstone rocks due to the low natural granulometry of these mineral species. Figure 10 shows the diffractogram of the Botucatu sandstone sample in black line. Additionally, the diffractograms of the quartz $SiO_2$ (PDF-33-116 - Tune Cell) and kaolinite $Al_2O_9SiO_2$ (IICOD9014999) patterns are shown in red and blue lines, respectively, in Figure 10.

As it may be observed in these diffractograms, the sandstone samples showed peaks related to both standards, indicating the presence of $SiO_2$ and $Al_2O_9SiO_2$, corroborating the results obtained in the measurements of X-Ray Fluorescence, where these elements are in the proportion of 76% $SiO_2$ and 20% $SiO_2$ e 20% de $Al_2O_9SiO_2$. In the diffractogram of the sandstone sample, no peaks relative to $Fe_2O_3$ were observed, probably due to its low concentration of 2.3%, determined by the Fluorescence technique.

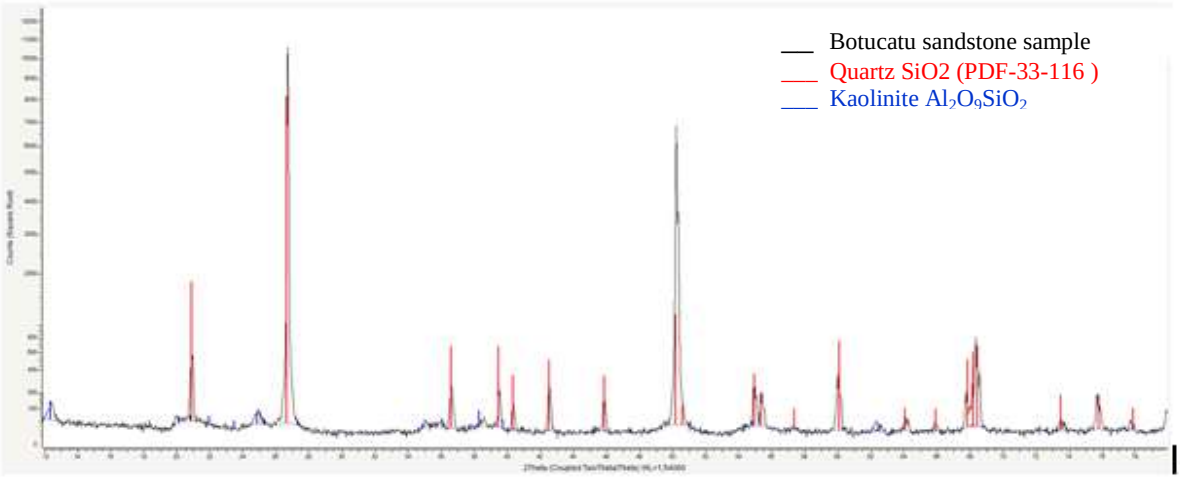


Figure 10. X-ray diffraction from the Botucatu sandstone sample

Fig. 11 shows the images of the sandstone sample obtained by optical microscopy, enlarged 40 and 100 times. Although the resolution of the image by the MO technique is lower than by MEV, the surface structure may be noticed. As observed, it presents characteristics of sandstone soil, having traces of clay and formed basically of minerals, that probably must be of predominance of quartz and kaolinite. The grains are typical of desert sand, that is, well selected. This characterizes good reservoirs.

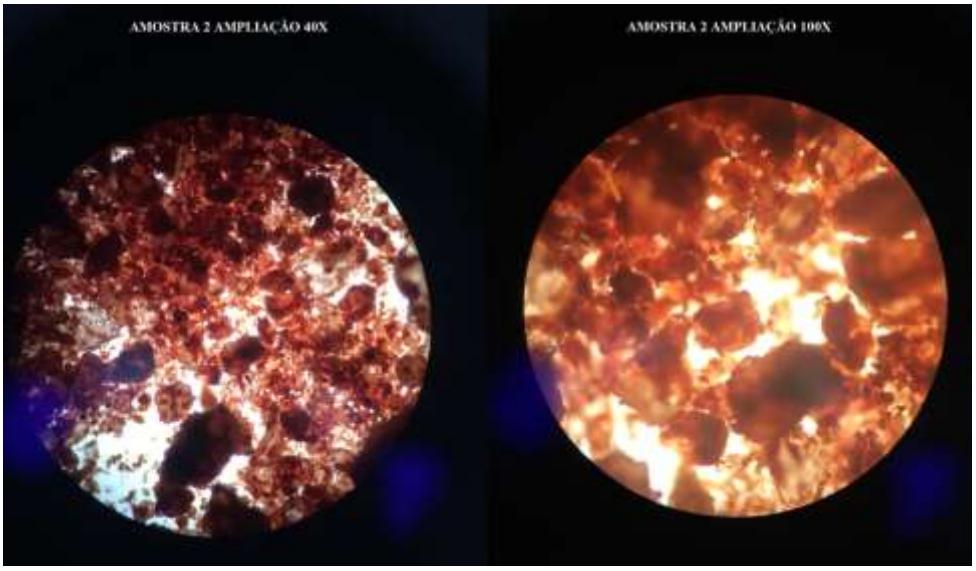


Figure 11. Images from the Botucatu Formation sandstone sample, with 40 and 100-fold magnification.

Figure 12 shows the images of the sandstone rock morphology obtained by SEM amplified 100 and 500 times, while Figure 13 shows the magnified images 1000, 1200, 1500, 2000 and 2500 times. The images obtained by SEM allow the structures in each granulometry to be evaluated.

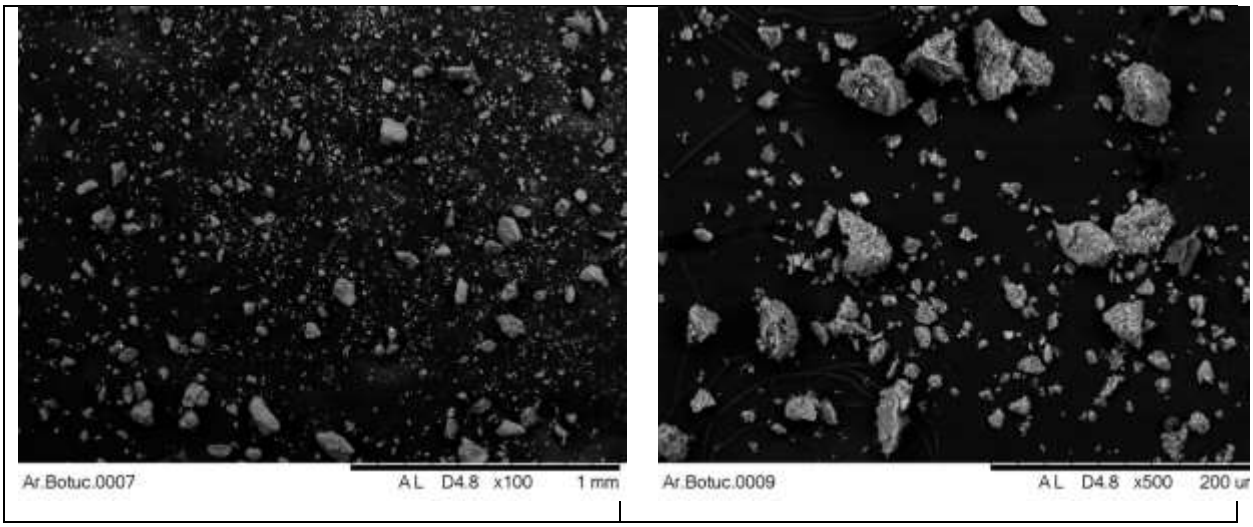


Figure 12. Botucatu sandstone images magnified 100 and 500 times.

In the enlarged image 100 and 500 times (Fig. 12), fine sand is observed and the nuclei, because they are dispersed, do not confer cement, confirming its characteristic of reservoir rock.

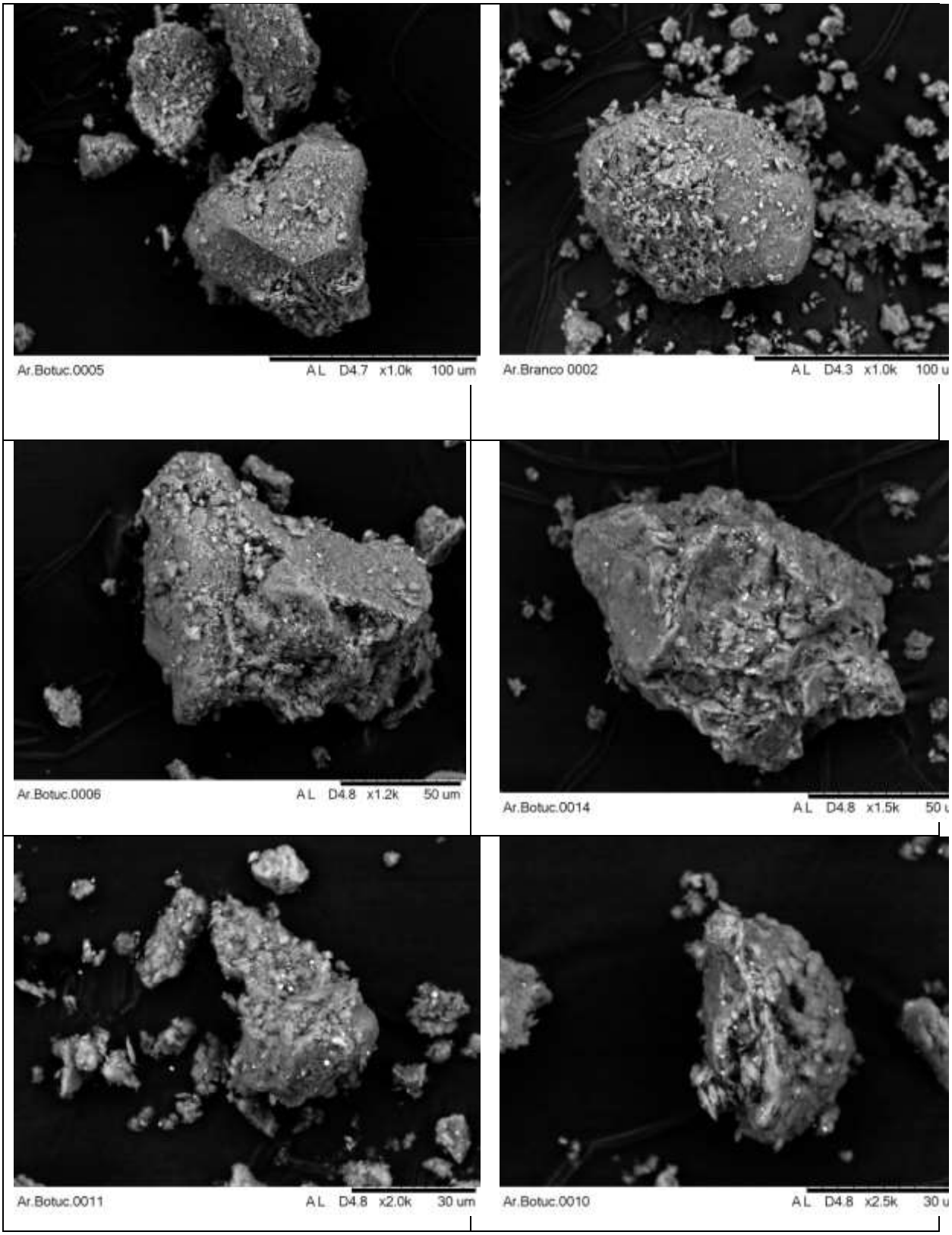


Figure 13. Botucatu sandstone images enlarged from Botucatu sandstone magnified 1000, 1200, 1500, 2000 and 2500 times.

It is possible to identify the structure of the oxide deposition layers, probably of $Al_2O_3$ and $Fe_2O_3$ in a probably quartz nucleus, in the images shown in Fig. 13 with greater magnification (magnification of 1000, 1200, 1500, 2000 and 2500 times).

## 3. CONCLUSIONS

The shear wave rate (Vs) was determined, associating to different rock parameters, such as dr y density ($\rho_d$), void index (e), moisture content (W), degree of saturation (S) and porosity ($\eta$). The permeability coefficient (k) obtained in the test was 3.34E-04 cm/s, and is consistent with the value of sandstone soil, originating from a reservoir rock. The test for achieving the plasticity limit indicated that the evaluated rock soil is not plastic. The sandstone analyzed by the X-ray fluorescence technique was predominantly composed of $SiO_2$ (76%) and $Al_2O_3$ (20%), followed by $Fe_2O_3$ (2.3%). The X-ray diffractograms of the sandstone samples showed relative peaks $SiO_2$ and $Al_2O_9SiO_2$ patterns, corroborating the results obtained in X-ray Fluorescence measurements. In the sandstone sample diffractograms, no $Fe_2O_3$ peaks were observed, probably due to its low concentration of 2.3%, determined by Fluorescence technique. SEM studies showed that the rocks did not have cementation in their structures, indicating that they are reservoir rocks, with potential for water storage.

## ACKNOWLEDGMENTS

The authors express their acknowledgment to CNEN, FAPESP and the IAEA for the financial support. The authors, Carlos Henrique de Mesquita, Margarida Mizue Hamada, Alexandre F. Veol, Diego V. S. Carvalho, Rodrigo S. dos Santos and Tarciano J. do Nascimento express their gratitude the CNPq for fellowships and Rafael A. Amadeu thank to CNEN,.

## REFERENCES

1. Bigarella, J. J. e Salamuni, R. (1967). The Botucatu Formation. (inglês) IN: J. J. Bigarella,, R.D. Becker, J.D.Pinto (eds). Problems in Brazilian Gondwana Geology. UFPR, Curitiba, p. 198-206
2. Caetano-Chag, M. R.; WU, F. T. (1992) Bacia do Paraná: Formações Pirambóia e Botucatu. IN: Congresso Brasileiro de Gelogia, 37. São Paulo. Roteiro de excursão ... São Paulo: Sociedade Brasileira de Geologia, 1992, n. 2 , p. 1-19.
3. Caetano-Chag, M. R.; Wu, F. T. (1993) A composição faciológica das formações Pirambóia e Botucatu no centroleste paulista e a delimitação do contato entre as unidades. IN: Simpósio de Cronoestratigrafia da Bacia do Paraná. 1., Rio Claro. Boletim de resumos. Rio Claro: Universidade Estadual Paulista, 1993, p. 93.
4. Caetano-Chang M.R., Wu F. 2003. Diagênese de arenitos da Formação Piramboia no centro leste Paulista. Revista Geociências, 22:33-47.
5. Carneiro, C.D.R. 2007. Viagem virtual ao Aqüífero Guarani em Botucatu (SP): Formações Pirambóia e Botucatu, Bacia do Paraná.

6. Chang, H. K. 2006. Utilização atual do Aquífero Guarani. In: Jornada Estadual Aquífero Guarani, 1, Botucatu, SP, 2006 (cd – rom).
7. Cormack, A.M. Representation of a function by its line integrals, with some radiological applications. J. Appl. Phys., v. 34, p. 2722 – 2727, 1963.
8. Gesicki, A. L. D. G. 2007. Evolução diagenética das Formações Pirambóia e Botucatu (Sistema Aquífero Guarani) no Estado de São Paulo. 2007. 175p. Tese (Doutorado) – Instituto de Geociências. Universidade de São Paulo.
9. Liu, J., Lozano-Perez, S., Karamched, P., Holter, J., Wilkinson A. J., Grovenor, C. R. M., Forescattered electron imaging of nanoparticles in a scanning electron microscopy, Department of Materials, University of Oxford, Parks Road, OX1 3PH, United Kingdom, 2019
10. Massoli, M. 2007. Caracterização litofaciológica das formações Pirambóia e Botucatu, em subsuperfície, no município de Ribeirão Preto (SP) e sua aplicação na prospecção de águas subterrâneas /Marcos Massoli. – Rio Claro : [s.n.], 2007.
11. Montanheiro, T. J., Artur A. C., Montanheiro F., Negri F. A., Gesicki A. L., Boggiani P. C. Investigação Tecnológica de arenitos silicificados da Formação Botucatu (NE do Paraná) para uso como rocha de revestimento. São Paulo, UNESP, Geociências, v. 30, n. 2, p. 237-251, 2011.
12. Morales, L.F.G., Hinrichs, R., Fernandes, L.A.A., A Técnica de Difração de Elétrons Retro-Espalhados (EBSD) em Microscópio Eletrônico de Varredura (MEV) e sua Aplicação no Estudo de Rochas Deformadas. Revista Pesquisas em Geociências, 34 (1): 19-34, Porto Alegre, 2007.
13. NBR 16434/2015, Amostragem de resíduos sólidos, solos e sedimentos - Análise de compostos orgânicos voláteis (COV) – Procedimento, ABNT, 2015
14. NBR 7180, Solo – Determinação do limite de plasticidade, ABNT, 2014.
15. Peterson, L. J., Mortillaro, C. A., Warner, B. P., Zahler, N. H., Portage, P. B., Hsieh, C. T., Solomon, L.A., Method for analysis using X-Ray Fluorescence,: ICAGEN, INC., DURHAM, NC (US), 2018, 25 p
16. Rocha, B.L. – 2017 - Caracterização e Aspectos Diagenéticos de Arenitos das Formações Botucatu e Piramboia no Centro-Norte do Estado do Paraná. Trabalho de Conclusão. Universidade Federal do Paraná, Curitiba – PR. 49p.
17. Santos, R. A, 2016 Estudo da influência de impurezas e da qualidade das superfícies em cristais de brometo de tálio para aplicação como um detector de radiação. Tese de Doutorado. Instituto de Pesquisas Energéticas e Nucleares, São Paulo – SP. 99p
18. Scapin, M. A., Aplicação da difração e fluorescência de Raios X (WDXRF): Ensaios em Argilominerais. Dissertação de Mestrado em Ciências na Área de Tecnologia Nuclear – Materiais. IPEN, 2003, 80 p.
19. Soares, P. C. (1972) Arenito Botucatu e Pirambóia no Estado de São Paulo. In: Congresso Brasileiro de Geologia, 26., Belém, Resumos. São Paulo: Sociedade Brasileira de Geologia, 1972, p. 250-251.